Photocatalytic removal of the cyanobacterium Microcystis aeruginosa PCC7813 and four microcystins by TiO2 coated porous glass beads with UV-LED irradiation.

PESTANA, C.J., PORTELA NORONHA, J., HUI, J., EDWARDS, C., GUNARATNE, H.Q.N., IRVINE, J.T.S., ROBERTSON, P.K.J., CAPELO-NETO, J. and LAWTON, L.A.

2020

Photocatalytic removal of the cyanobacterium *Microcystis aeruginosa* PCC7813 and four microcystins by TiO_2 coated porous glass beads with UV-LED irradiation

Carlos J. Pestana[a*], Jolita Portela Noronha[a,b], Jianing Hui[c], Christine Edwards[a], H. Q. Nimal Gunaratne[d], John T.S. Irvine[c], Peter K.J. Robertson[d], José Capelo-Neto[b], Linda A. Lawton[a]

[a] School of Pharmacy and Life Sciences, Robert Gordon University, Aberdeen, United Kingdom
[b] Department of Hydraulic and Environmental Engineering, Federal University of Ceará, Fortaleza, Brazil
[c] School of Chemistry, University of St. Andrews, St. Andrews, United Kingdom
[d] School of Chemistry and Chemical Engineering, Queen's University, Belfast, United Kingdom

*Corresponding author: c.pestana@rgu.ac.uk

Keywords: Cyanobacteria, Photocatalysis, Cyanotoxins, Water Treatment, Titanium Dioxide, UV-LED

Highlights

- Photocatalytic inhibition of *M. aeruginosa* PCC7813 (7.6×10^5 cells mL^{-1} d^{-1})
- 74% removal of four microcystins (intra- and extracellular)
- Porous glass beads made from recycled glass used as catalyst support
- UV irradiance supplied by low energy UV (365 nm) emitting LEDs

Graphical Abstract

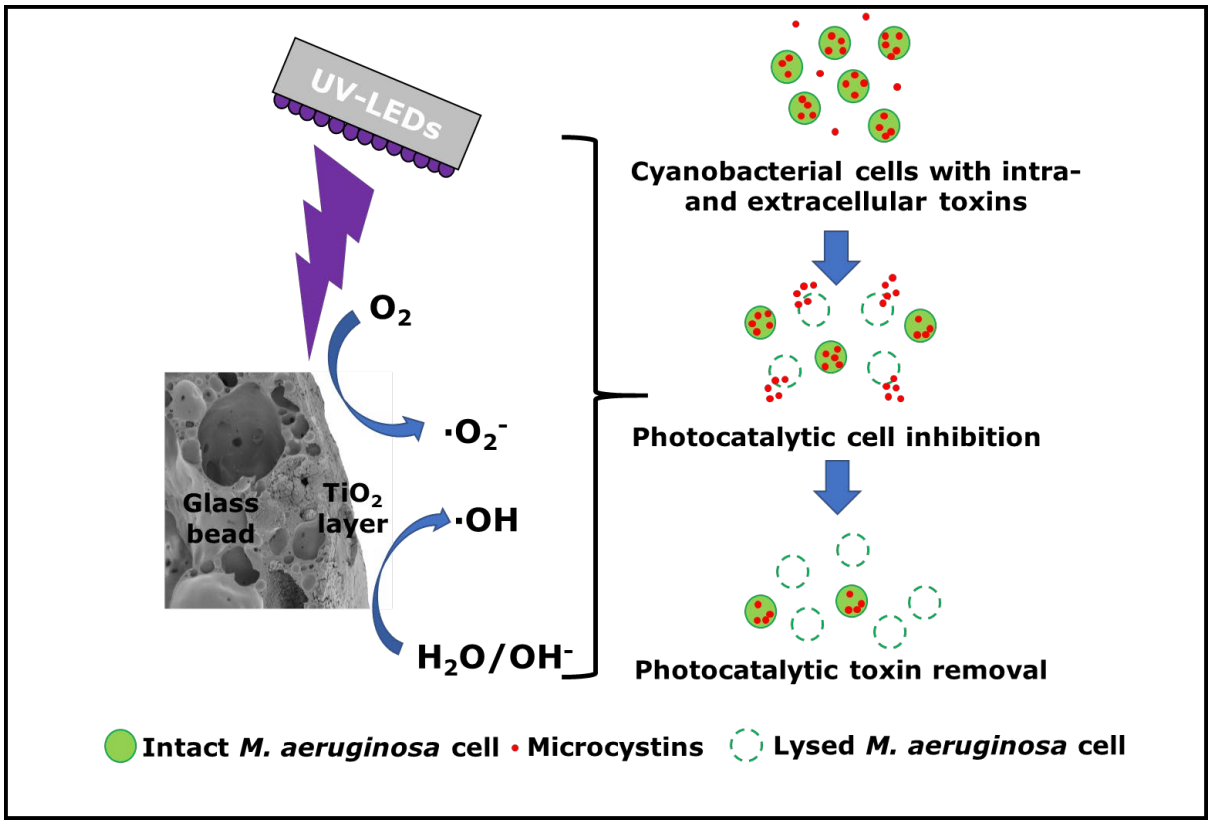

Abstract

Cyanobacteria and their toxic secondary metabolites are a challenge in water treatment due to increased biomass and dissolved metabolites in the raw water. Retrofitting existing water treatment infrastructure is prohibitively expensive or unfeasible, hence 'in-reservoir' treatment options are being explored. In the current study, a treatment system was able to photocatalytically inhibit the growth of *Microcystis aeruginosa* and remove released microcystins by photocatalysis using titanium dioxide coated, porous foamed glass beads and UV-LEDs (365 nm). A 35% reduction of *M. aeruginosa* PCC7813 cell density compared to control samples was achieved in seven days. As a function of cell removal, intracellular microcystins (microcystin-LR, -LY, -LW, and -LF) were removed by 49% from 0.69 to 0.35 µg mL^{-1} in seven days. Microcystins that leaked into the surrounding water from compromised cells were completely

removed by photocatalysis. The findings of the current study demonstrate the feasibility of an in-reservoir treatment unit applying low cost UV-LEDs and porous foamed beads made from recycled glass coated with titanium dioxide as a means to control cyanobacteria and their toxins before they can reach the water treatment plant.

1. Introduction

Cyanobacteria are well known to form blooms in nutrient-rich waters, including drinking water reservoirs. High cell densities challenge water treatment systems by reducing the run time of filters leading to an increased demand of treatment chemicals such as coagulants and disinfectants (De Julio *et al.*, 2010). This problem is often further acerbated by the release of toxic and/or noxious metabolites produced by the cyanobacteria, further challenging water treatment plant operators and decreasing water security *(*Chow *et al.,* 1999*;* Drikas *et al.,* 2001*;* Velzeboer *et al.*, 1995). The most commonly reported cyanobacterial toxic metabolites are the microcystins. To date at least 247 microcystin congeners have been described (Spoof and Catherine, 2017). The toxicity of microcystins has been recognized as a global issue with the World Health Organisation setting a recommended maximum allowable limit of 1 μg L^{-1} in drinking water (WHO, 2017).

Retro-fitting water treatment plants with improved and advanced technology is often prohibitively expensive and/or physically challenging, hence alternative treatment technologies such as in-reservoir treatment need to be explored. The application of algaecides in the reservoir is the simplest form of in-reservoir treatment but studies have shown the negative effects of this practice, such as toxicity to non-target organisms, development of bacterial resistances, increase

of potentially toxic/noxious dissolved metabolites and precursors of disinfection by-products (Bishop *et al.*, 2017; García-Villada *et al.*, 2004; Greenfield *et al.*, 2014; Jančula and Maršálek, 2011).

In recent years, advanced oxidation processes, including titanium dioxide (TiO_2) photocatalysis have been demonstrated to control cyanobacteria and their secondary metabolites. Successful removal of cyanobacterial toxins by TiO_2 nanoparticulate photocatalysis have been reported by a number of studies (Cornish *et al.*, 2000; Liu *et al.*, 2009; Pelaez *et al.*, 2011), especially for the elimination of the commonly occurring group of cyanobacterial toxins, the microcystins. One of the most critical technical challenges that has hampered the application of photocatalysis in water treatment is the removal of the nanoparticulate TiO_2 materials following treatment. The post treatment recovery of TiO_2 is not only a technical challenge but also has ecotoxicological health implications. It has been demonstrated that nanoparticulate TiO_2 can bioaccumulate and damage biota (Heinlaan *et al.*, 2008; Wang *et al.*, 2007; Zhu *et al.*, 2010). Further, the application of nanoparticulate TiO_2 represents a health hazard to operators if inhaled (Grassian et al., 2007). To avoid the problems of free nanoparticulate TiO_2, immobilization of the photocatalyst onto a robust carrier matrix is preferable. Matrices such as activated carbon, metal particles, and glass have been explored, each with inherent advantages and disadvantages (Kinley et al., 2018; Liu et al., 2007; Pestana *et al.*, 2015). Several design parameters have to be considered when applying immobilized TiO_2 in a water treatment context. For example, cyanobacteria occupy different positions in the water column, depending on species and time of the day (Varuni *et al.*, 2017). Thus, to ensure maximum efficiency of immobilized TiO_2, an even distribution throughout the water column is desirable. Surface floating matrices will not

reach cyanobacteria deeper in the water column and likewise heavier matrices that sink will miss cyanobacteria higher up in the water column. The use of semi-bouyant foamed glass beads allows for even distribution in the water column. Additionally, the use of low-cost (ca. USD 0.30 per LED), long life (approximately 100,000 working hours), waterproof UV (365 nm) emitting LEDs to activate TiO_2 would solve a further technological challenge in the application of this *in-situ* treatment system, as in the past supplying cost-effective UV irradiation of the required wavelength has been problematic. While in recent years solar light-driven photocatalysis has been explored for the removal of contaminants of emerging concern, including cyanobacteria and their toxins, the application of this technology at scale suffers from drawbacks compared to the use of for example UV-LEDs (Fagan et al., 2016). There are two major drawbacks to this technology, one is the need to modify TiO_2 to shift its activity into the visible light range, usually achieved doping with other materials such as noble metals, carbon, or nitrogen (Wang et al., 2017, Fotiou et al., 2013). This would increase the cost of the treatment as additional steps and materials are required in the catalyst preparation. The other drawback of solar light-driven catalysis is that sunlight hours vary across the globe and that it is only available for a maximum of 12 h per day, thus rendering a purely solar light-driven treatment system inactive overnight. Recently, we have shown the feasibility of such a system for the photocatalytic removal of microcystin-LR (Gunaratne *et al.*, 2020). Applying a similar technology using TiO_2 coated porous glass beads and UV-emitting LEDs, we now present a bench scale proof-of-principle in-reservoir treatment system that aims to inhibit and eliminate cyanobacteria while simultaneously removing toxins that are released and is energy efficient, thus can be maintained in continuous use to limit cyanobacterial biomass and

dissolved metabolites entering water treatment plants. It is envisaged that the pre-treatment system operates continuously avoiding the formation of intense blooms and keeping the cyanobacterial biomass at a level that allows the conventional water treatment process to completely remove any remaining cyanobacteria, while at the same ensuring that no dissolved toxins enter the plants that are ill equipped to remove dissolved contaminants, rather than a point treatment used when cell numbers or toxin concentrations exceed national threshold levels.

2. Materials and Methods

2.1 Reagents

All reagents for the preparation of artificial fresh water (AFW) and cyanobacterial culture medium BG-11 were of reagent grade, obtained from Fisher Scientific (UK), and used as received. Acetonitrile and methanol were of HPLC grade and obtained from Fisher Scientific (UK). Ultrapure water (18.2 MΩ) was provided by a PURELAB© system (ELGA Veolia, UK). Isoton II Diluent (Beckman Coulter, USA) was used for cell enumeration and biovolume determination.

2.2 Cyanobacterial cell culture

M. aeruginosa PCC7813 was originally obtained from the Pasteur Culture Collection (France) and cultured in sterilized BG-11 medium (Stanier *et al.*, 1971), at 22±1 °C with a 12h/12h light dark cycle at 20 µmol photons m^{-2} s^{-1} under aseptic conditions. *M. aeruginosa* PCC7813 produces four main microcystin analogues (MC-LR, MC-LY, MC-LW, and MC-LF) and does not contain gas vesicles.

2.3 Preparation of TiO_2 coated recycled porous glass beads

Porous recycled foamed glass beads (1-4 mm diameter, Poraver, Germany) were sieved to achieve > 2 mm, then washed with acetone, followed by deionised water in a sonication bath (Scientific Laboratory Supplies Ltd., UK) and dried in an oven at 80 °C for 18 h. After this pre-treatment, beads were coated with titanium dioxide (P25, Rutile/Anatase: 85/15, 99.9 %, 20 nm particle size; Degussa Evonik, Germany) according to a method by Mills *et al.* (2006) with adaptations. In short, a slurry of P25 and water is prepared into which the pre-treated glass beads are submerged. Coated beads are removed from the slurry and allowed to dry, followed by calcination at 550 °C for 3h. Each coating procedure deposits approximately 2% (w/w) of TiO_2 onto the beads. Coatings are repeated until approximately 10% (w/w) of TiO_2 on the beads was achieved. Characterization of the beads and the coating is recorded in the supplementary material (S1 and figure S1).

2.4 Photocatalytic removal of *M. aeruginosa* PCC7813 and microcystins

Artificial fresh water (AFW) was used as an experimental matrix in the photocatalysis investigation, and was prepared according to Akkanen and Kukkonen (2003) by dissolving $CaCl_2$ (11.8 mg L^{-1}), $MgSO_4$ (4.9 mg L^{-1}), $NaHCO_3$ (2.6 mg L^{-1}) and KCl (0.2 mg L^{-1}) in ultrapure water. A three-week-old culture of *M. aeruginosa* PCC7813 was diluted in AFW to achieve a final cell density of 15 x 10^6 cells mL^{-1}. TiO_2 coated beads (700 mg, equivalent to 0.2% (w/v) TiO_2) were placed in glass mesh pods (70 mm x 10 mm diameter) and placed into 40 mL glass bottles (95 mm x 22 mm diameter) into which 30 mL of the cell suspension was added. Three replicates containing the coated beads was irradiated by a 550 cm^2 UV-LED panel with 90 individual UV-LEDs (AT

Technologies, UK) providing 2.8 µmol photons m^{-2} s^{-1} (2.1 mW s^{-1}) at 365 nm and at 100 mm distance (figure 1). Another three replicates, not containing titanium dioxide coated beads was prepared at the same distance from the UV-LEDs functioning as a UV control. While a third set of replicates with TiO_2 coated beads was set up outside of the area of irradiation of the UV-LED panel to act as a no-UV control. Typically, in photocatalysis the dark/no-UV control is performed in complete darkness; however, cyanobacteria are photosynthetic organisms that would not survive the duration of the experiment without light, hence this third set of replicates was maintained in ambient light (no UV irradiation at 13 µmol s^{-1} m^{-2} cool fluorescent irradiation). To maintain clarity 'TiO_2-control' will be used throughout to identify samples that contain TiO_2 coated glass beads, but are not exposed to UV irradiation. All samples were sparged at 1.5 L min^{-1} with sterile ambient air. After taking a zero-time sample, each replicate was sampled (1.1 mL) daily.

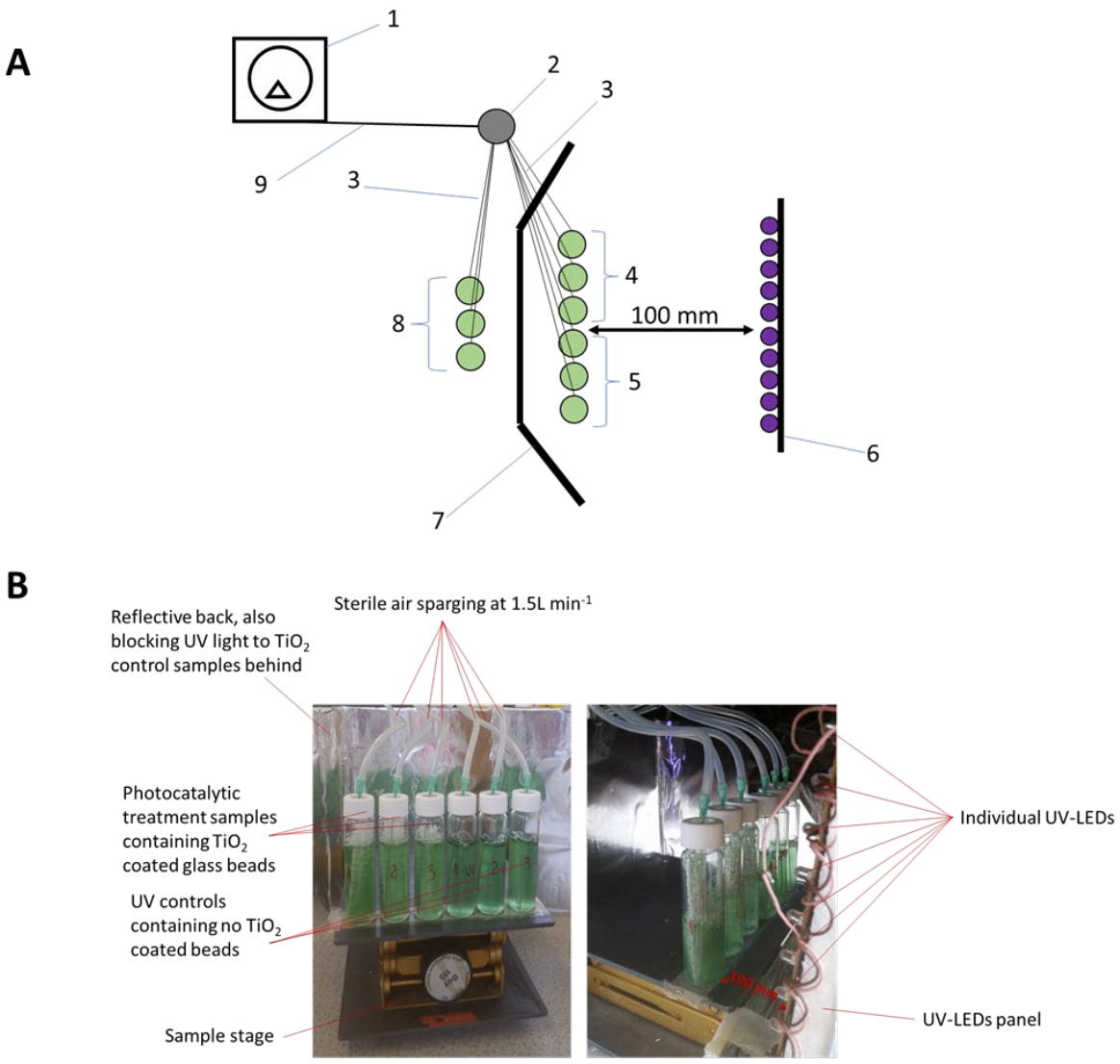

Figure 1: A) Schematic diagram of the UV-LED photocatalytic experimental design (top-down view). 1- air pump, 2- air distribution hub to achieve equal air pressure across all samples, 3- silicone tubing of equal length, 4- TiO_2/UV treatment samples in triplicate, 5- UV control samples in triplicate, 6- UV-LED panel with 90 UV-LEDs (365 nm, 67.5 mW total output) in 9 rows of 10 LEDs; output at 100 mm 2.6 mW s^{-1}, 7- reflective surface; also blocking UV irradiation from LED panel to TiO_2-controls (8), 8- TiO_2-control samples in triplicate, 9- silicone tubing. B) Photographic representation of the reactor and the TiO_2/UV and UV control samples.

2.5 Sample analysis

2.5.1 Cell enumeration and sample pre-treatment

For cell enumeration, cell volume determination, and determination of the average cell diameter of *M. aeruginosa* PCC7813, 0.1 mL of each sample was diluted in 20 mL of Isoton II diluent and analysed by a Multisizer (Beckman

Coulter, USA). For this a 50 µm aperture was used, allowing the determination of particles sized between 1 and 30 µm, particles ranging in size from 2.8 to 6.9 µm were considered intact cells based on published data of cell size ranges for *M. aeruginosa* (Harke *et al.*, 2016; Komárek and Komárková, 2002). This cut-off had to be introduced to ensure that cell fragments smaller than 2.8 µm are not considered cells which would artificially increase the cell densities. For microcystin analysis, the remaining 1 mL of each sample was centrifuged (13000 G) in microcentrifuge tube (1.5 mL) for 10 min to separate cells and medium. The supernatant was evaporated to dryness on an EZ-II Evaporator (Genevac, United Kingdom). The cell pellet was stored at -20 °C until further processing. Prior to analysis, aqueous methanol (80 %) was added to the cell pellets which were subsequently placed in a dispersive extractor for 5 minutes at 2500 rpm and then centrifuged (13000 G). The supernatant was analysed to determine intracellular toxin. The dried extracellular component was also resuspended in aqueous methanol (80%, 150 µL), vortexed and centrifuged (13000 G). The intra- and extracellular microcystins were analysed by HPLC.

2.5.2 High performance liquid chromatography analysis of microcystins

Chromatographic separation of microcystin analogues was carried out using a 2965 separation module with a Symmetry C18 column (2.1 x 150 mm, 5 µm particle size) and a 2996 photodiode array (PDA) detector. Mobile phases were ultrapure water (18.2 MΩ) and acetonitrile both with 0.05% trifluoroacetic acid. Separation was achieved with a linear gradient from 35 to 70% organic phase over 25 min followed by an organic solvent wash (100%) and re-establishment of starting conditions. Column temperature was 40 °C. Scanning range for the

PDA was 200 to 400 nm, with microcystins integrated at 238 nm. The limit of quantification of this method was 5 ng mL^{-1}.

2.5.3 Statistical analysis

All values shown are mean of triplicate treatments with error of one standard deviation. For statistical significance testing results were analyzed using one-way ANOVA. The significance level was set to $p>0.05$ to identify significant differences between results.

3. Results and Discussion

3.1 Photocatalytic removal of *M. aeruginosa* PCC7813

The removal of *M. aeruginosa* PCC7813 in a photocatalytic reactor with TiO_2 coated porous glass beads and UV-LED irradiation was initially investigated. Over the course of seven days treatment the cell concentration of *M. aeruginosa* PCC7813 increased significantly in both controls, UV with no catalyst and no UV irradiation ($p<0.05$ each), achieving 32 and 34 x 10^6 cells mL^{-1} respectively, representing a per cent increase of 213 and 226%. There was no statistical difference between the UV- and the TiO_2-controls ($p>0.05$). No effect of the UV only control would be expected as the UV light emitted by the UV-LED is comparatively low in energy at 2.6 mW s^{-1} and the emitted wavelength is insufficient to be germicidal (germicidal wavelength <254 nm; Ou *et al.*, 2012). On the other hand, in the treatment samples the initial cell concentration (15 x 10^6 cells mL^{-1}) was significantly reduced to 10 x 10^6 cells mL^{-1} (35%, $p=0.00004$) when compared to the TiO_2-control (figure 2). The biovolume of the *M. aeruginosa* PCC7813 culture also decreased over the course of the experiment (66% of the TiO_2- control), which corresponds to and corroborates

the observed decrease in cell density. There was no statistical difference between the two controls with respect to the cell volume (p>0.05). The diameter of the intact cells (2.8-6.5 μm) did not significantly change (p>0.05) from either the initial cell size at time zero or after seven days treatment when compared to either control (UV with catalyst and no UV irradiation). This indicates that the treatment fragmented the cells into particles smaller than 2.8 μm rather than affect the cell diameter since the mean cell diameter did not change. Cell fragmentation during photocatalytic treatment was also observed by Wang *et al.* (2017) where *M. aeruginosa* (strain 913 from Wuhan Institute of Hydrobiology) cells were treated with floating, expanded perlite particles that were coated with F-Ce doped TiO_2.

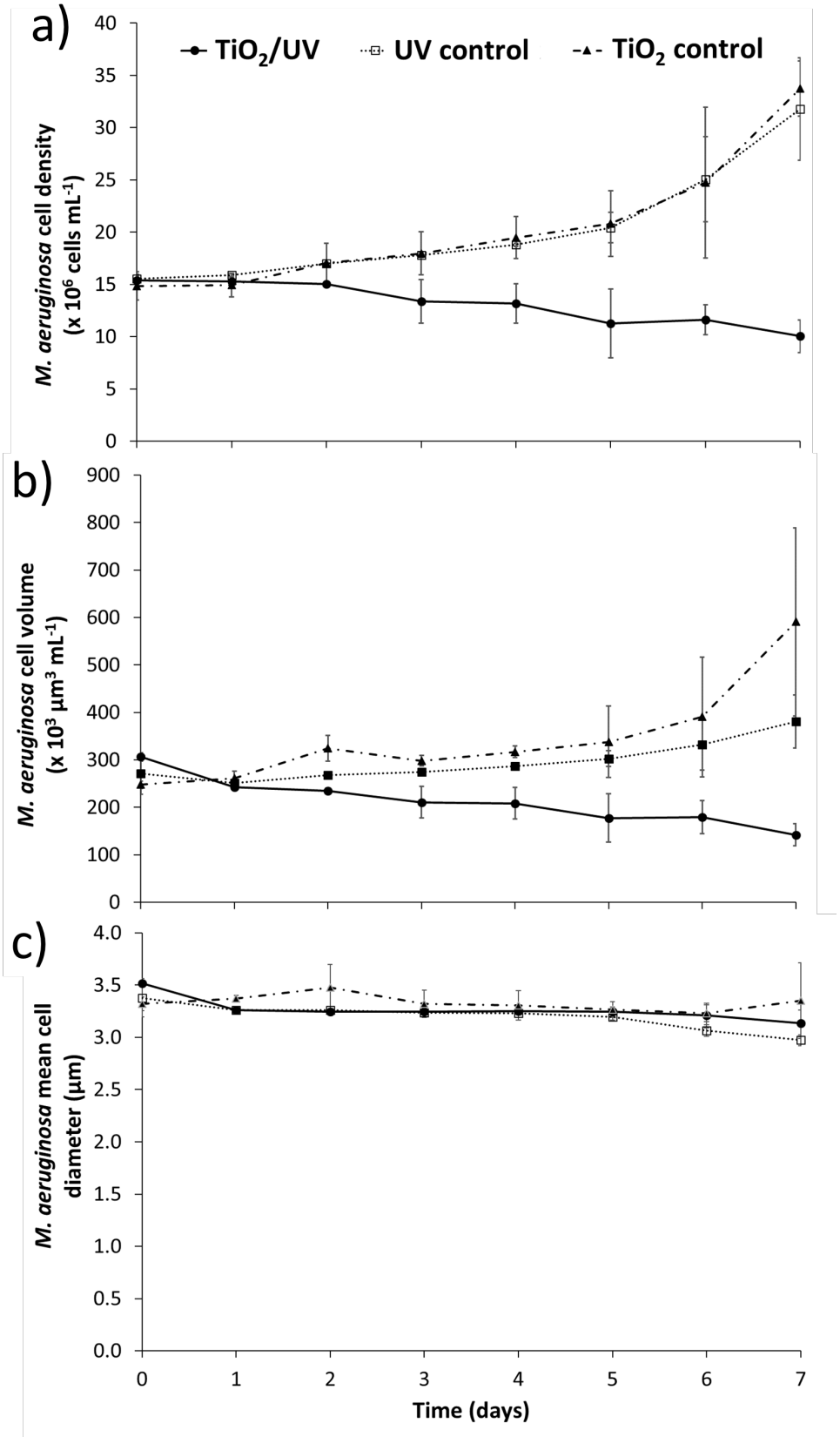

Figure 2: a) Removal of *M. aeruginosa* PCC7813 cells by photocatalysis using TiO_2 coated porous glass beads over a seven-day period under 2.8 µmol photons m^{-2} s^{-1} at 365 nm (2.6 mW s^{-1}) at 100 mm distance, as well as the effect of the treatment on *M. aeruginosa* PCC7813 b) cell volume, and c) mean cell diameter. (*n*=3, Error=1SD)

From 48 h onwards, a decline in cell density was observed for the treatment with TiO_2/UV (figure 2a). Other studies have reported the inhibition of *M. aeruginosa* growth by TiO_2 photocatalysis in one hour (Liao *et al.*, 2009; Pinho *et al.*, 2015), however, there are marked differences in the application of the TiO_2 photocatalysis in terms of light source, *M. aeruginosa* strain, and presentation of TiO_2. The UV-LED panel employed in the current investigation had a total output of 67.5 mW (with each individual LED having an output of 750 µW, and the panel having a total of 90 LEDs) providing a very low energy input into the system. By comparison Pinho *et al.* (2015), who investigated the removal of *M. aeruginosa* LEGE 91094 (IZANCY-A2) with particulate TiO_2, used simulated solar irradiation at a UV equivalent of 44 W m^{-2}, and Liao *et al.* (2009), who investigated the effect of silver-doped TiO_2 particulates on an unspecified *M. aeruginosa* strain, used a UV-C lamp with 4 W output at 253.7 nm. The UV-LEDs (67.5 mW) deployed in the current investigation use almost sixty times less energy than the 4 W lamp used in the other study. An additional advantage of employing LEDs is their longer life span in comparison to light bulbs, ca. 100,000 h compared to ca. 8,000 to 25,000 h for other UV irradiation sources (Heering, 2004). Furthermore, while rapid cell death is recorded when nanoparticulate TiO_2 is used, the removal of catalyst has been a barrier to deployment of this technology. A particular advantage of the current system is the use of immobilized TiO_2. While the reactive surface area is markedly reduced compared to particulate catalyst systems, immobilized catalyst offers a much more facile post-treatment separation of catalyst and water compared to (nano)particulate TiO_2. In addition, most of these other studies which investigated the inhibition of *M. aeruginosa* by TiO_2 photocatalysis, used modified TiO_2 composite materials. Liao and co-workers (2009) used Ag-doped TiO_2 and Wang *et al.* (2017) used F-

Ce-doped TiO_2 further increasing the photocatalytic activity compared to TiO_2 alone. The doping of TiO_2 offers the advantage of shifting reactivity into the visible spectrum, however, this has to be weighed against the cost of the doping material and the complexity of preparation. Additionally, the intended application has to be considered. The current design is aimed at continuous operation within a reservoir to ease the burden on the water treatment process within a treatment plant. Thus, materials used need to be plentiful, economically affordable, and easy to obtain, which is not the case when doping with, for example, noble metals.

The UV irradiation (365 nm) alone had no observable effect on the cell number, cell volume, or cell diameter (figure 2), which was what might have been expected since antimicrobial UV treatments tend to employ irradiance in the UV-C spectrum of a wavelength of 260 nm and below (Wolfe, 1990). This was demonstrated in the Liao *et al.* (2009) study where approximately 12% difference in the chlorophyll *a* content between an untreated and the UV(C) controls was observed.

3.2 Photocatalytic removal of four microcystin congeners

The strain of *M. aeruginosa* PCC7813 used in the current investigation produces four main microcystin congeners (MC-LR, -LY, -LW, and -LF). During the photocatalysis of *M. aeruginosa* PCC7813 both the intracellular (figure 3) and extracellular (figure 4) microcystin concentrations were monitored. As microcystins are usually encountered in the intracellular space until cell integrity is compromised and the intracellular toxins leak into the surrounding water, monitoring the intracellular concentration during photocatalysis can be used as a proxy measurement of cell integrity. The distribution of the four congeners at

328 the start of the experiment was MC-LR 58%, MC-LY 9%, MC-LW 14%, and MC-
329 LF 19% of the total intracellular microcystin concentration. A significant
330 (p=0.0009 to 0.045) decrease of intracellular toxin concentration was observed
331 for all four microcystin congeners over the course of seven days (figure 3)
332 during photocatalytic treatment. Combined intracellular microcystin content
333 decreased by 49% from 0.69 to 0.35 μg mL^{-1}. Individually the concentrations for
334 MC-LR, -LY, -LW, and -LF decreased by 53, 34, 60, and 54% respectively from
335 the initial concentration present in the cells. The profile of different intracellular
336 microcystin variants at the end of the seven-day experiment remained largely
337 unchanged, with MC-LR remaining the main congener produced (54%), followed
338 by MC-LF (23%) and MC-LY and MC-LW (11% each). There was no statistical
339 difference *viz* the intracellular toxin concentration in either of the two controls
340 ($p>0.05$). Compared to the TiO_2 and UV with no catalyst controls the
341 concentration of the total intracellular microcystin in the treated samples was
342 reduced by 67% with individual concentrations for MC-LR, -LY, -LW, and -LF
343 decreased by 74, 50, 68, and 71% respectively. It is predicted that decrease in
344 cell density and toxins concentration would continue and be maintained at a low
345 level if this treatment system is used *in-situ* in a reservoir.

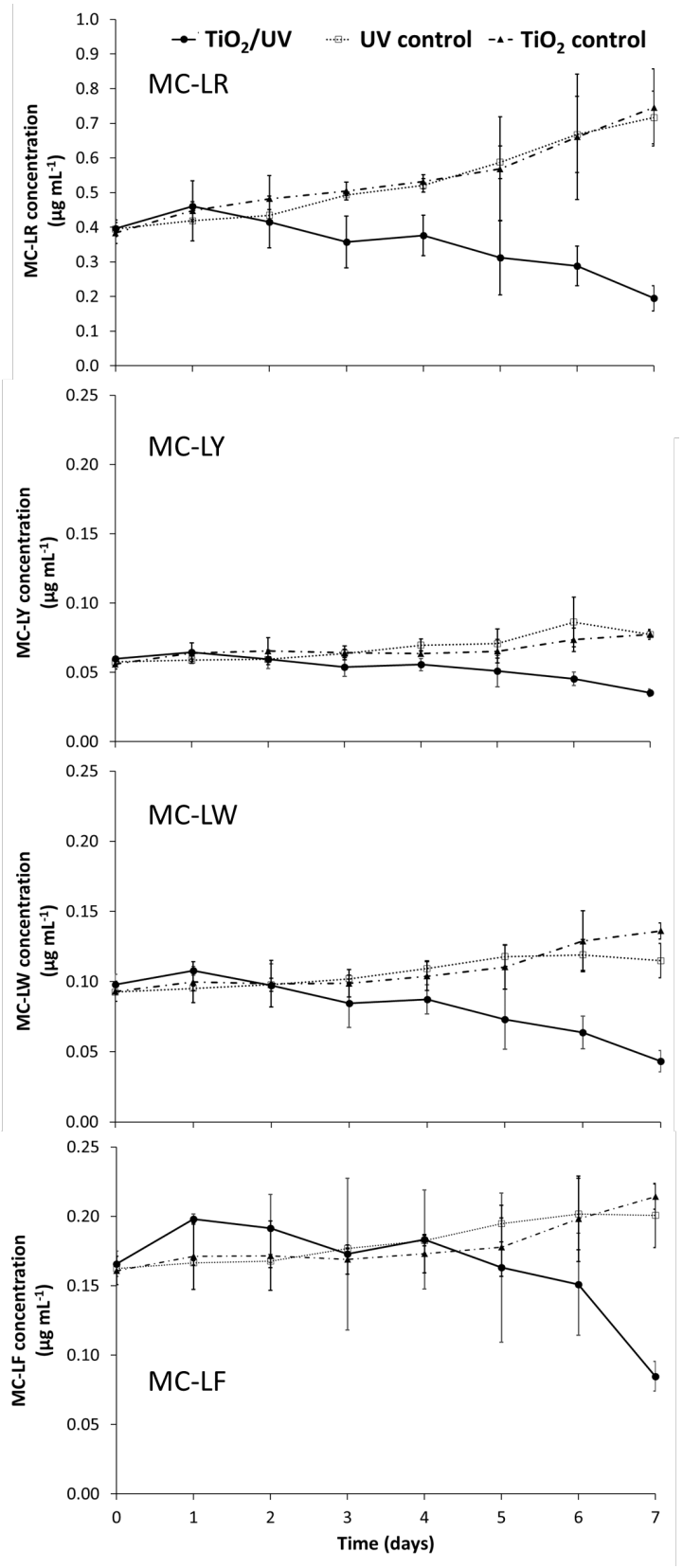

346

347 **Figure 3:** Removal of the four main intracellular microcystin analogues (MC-LR, MC-LY,
348 MC-LW, MC-LF) produced by *M. aeruginosa* PCC7813 during a seven-day photocatalytic
349 treatment with TiO_2 coated porous foamed recycled glass beads and UV-LED provided UV
350 irradiation at 2.8 µmol photons m^{-2} s^{-1} at 365 nm (2.6 mW s^{-1}) at a distance of 100 mm.
351 (*n*=3, Error=1SD)

For most of the congeners the amount of toxin per cell decreased (table 1), which is indicative that some of the cells detected by the particle counter were damaged, but had not yet completely fragmented. Zilliges and co-workers (2011) have observed that intracellular microcystins concentrations decrease as a response to oxidative stress. In their study Zilliges *et al.* (2011) were able to observe intracellular microcystins bind to intracellular proteins in the presence of hydrogen peroxide (0.34 mg L^{-1}). Hydrogen peroxide is a strong oxidizing agent and under UV irradiation hydrogen peroxide can lead to the creation of hydroxyl radicals, an even stronger oxidizing agent. Thus, the oxidative stress response of *M. aeruginosa* exposed to hydrogen peroxide may be comparable to the stress response to TiO_2 photocatalysis (where hydroxyl and superoxide radicals are created), indicating that the decrease in intracellular microcystin concentrations could also be caused by microcystins binding to intracellular proteins although this would require further investigation.

Table 1: Reduction of intracellular microcystin congener concentration in *M. aeruginosa* PCC7813 after seven days of treatment in a photocatalytic reactor under UV-LED irradiation (at 2.8 µmol photons m^{-2} s^{-1} at 365 nm (2.6 mW s^{-1})) at 100 mm distance in the presence of TiO_2 coated porous glass beads. (*n*=3, Error=1SD).

MC congener	Time 0 (fg $cell^{-1}$)	Time 7d (fg $cell^{-1}$)	Per cent reduction
MC-LR	25.8 ± 2	19.4 ± 2	25*
MC-LY	3.8 ± 0.1	3.5 ± 0.4	8
MC-LW	6.4 ± 0.4	4.3 ± 0.6	32*
MC-LF	10.8 ± 0.7	8.5 ± 0.8	21*

*difference significant (p>0.05)

When the cell integrity of microcystin-producing cyanobacteria is compromised by oxidative processes, the intracellular organic material leaks into the surrounding water, including any microcystins (Daly *et al.*, 2007). Therefore, it is important that water treatment systems either avoid compromising cell integrity or, failing that, the system should also be able to remove microcystins that are

379 released into the water. Failing to remove the dissolved organic matter,
380 including microcystins, acerbates the challenges faced by water treatment
381 processes, as conventional water treatment is more suited to the removal of
382 particulate and colloidal than dissolved components (Chow *et al.*, 1999; Li *et al.*,
383 2012). In the current investigation, extracellular concentrations of the four main
384 microcystin congeners produced by *M. aeruginosa* PCC7813 were also monitored
385 (figure 4).
386
387
388

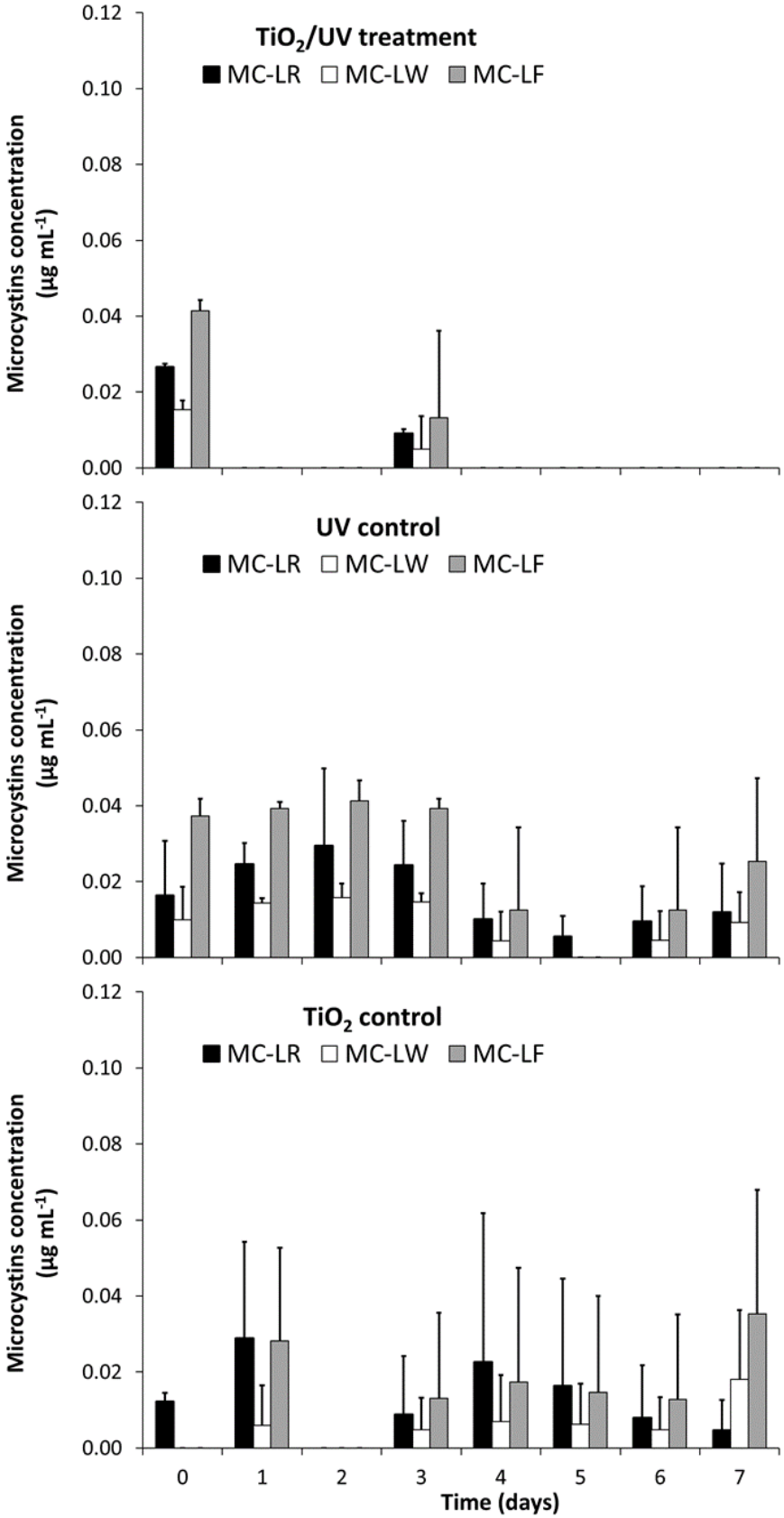

Figure 4: Extracellular microcystins (MC-LR, MC-LW, MC-LF) produced by *M. aeruginosa* PCC7813 during a seven-day photocatalytic treatment with TiO_2 coated porous glass beads and UV-LED provided UV irradiation at 2.8 µmol photons m^{-2} s^{-1} at 365 nm (2.6 mW s^{-1}) at 100 mm distance. (*n*=3, Error=1SD)

At the start of the experiment, relatively low concentrations (0.02-0.04 µg mL^{-1}) of extracellular MC-LR, MC-LW, and MC-LF were detected, while no extracellular MC-LY was detected. Over the course of seven-day photocatalytic treatment, the extracellular microcystin concentrations remained low, not exceeding 0.05 µg mL^{-1} in the treated samples, and were completely undetectable after day four of the UV/TiO_2 treatment. As the intracellular microcystins concentrations decrease due to loss of structural integrity of the cyanobacterial cells, extracellular toxin concentrations should increase, however this was not observed in the photocatalytically treated samples. Instead the intracellular microcystins were photocatalytically decomposed once they were released into the water. The efficacy of photocatalytic removal of dissolved microcystins has been demonstrated previously (Gunaratne *et al.*, 2020; Lawton *et al.*, 2003; Liu *et al.*, 2009; Pestana *et al.*, 2015). The decreased microcystin concentrations in the TiO_2-control compared to the UV only control can be explained with adsorption of the microcystin congeners onto the surface of the TiO_2 layer on the glass beads, as previously observed (Pestana *et al.*, 2015). The sum of the intracellular and extracellular microcystin concentrations of the TiO_2-control represents the total microcystin. Comparing this to the total microcystins of the photocatalytically treated samples allows the determination of the individual removal of the different microcystin congeners (table 2).

Table 2: Reduction of total microcystins (intra- and extracellular) produced by *M. aeruginosa* PCC7813 after seven days of treatment in a photocatalytic reactor under UV-LED irradiation (2.8 µmol photons m^{-2} s^{-1} at 365 nm (2.6 mW s^{-1})) at 100 mm distance in the presence of TiO_2 coated porous glass beads. (*n*=3, Error=1SD)

MC congener	Mean total microcystins TiO_2 control (µg mL^{-1})	Mean total microcystins photocatalytic treatment (µg mL^{-1})	Mean Δ total microcystins time 7d (µg mL^{-1})	Mean per cent reduction total microcystins
MC-LR	0.79 ± 0.04	0.19 ± 0.04	0.6 ± 0.07	76 ± 6
MC-LY	0.08 ± 0.01	0.04 ± 0.01	0.04 ± 0.01	55 ± 3
MC-LW	0.15 ± 0.02	0.04 ± 0.01	0.12 ± 0.01	72 ± 2
MC-LF	0.25 ± 0.03	0.08 ± 0.01	0.17 ± 0.03	66 ± 5
Combined	1.28	0.35	0.93	73

In the control samples (UV with no catalyst and TiO_2 with no UV) there were no cell-disrupting processes occurring which would lead to the liberation of microcystins. Thus, as expected, the extracellular microcystins concentrations (MC-LR, -LW, -LF) remained relatively consistent in both control samples over the course of seven days. Lack of cellular disruption is evidenced by the increase in cell numbers over the course of the seven days (figure 2) and intracellular microcystin concentrations (figure 3) in the TiO_2-control. The doubling rate of *M. aeruginosa* PCC7813 in the TiO_2-control is approximately seven days (from $1.5x10^6$ at time 0 to $3.4x10^6$ cells mL^{-1} at time 7 d). Wilson and co-workers (2006) report the average doubling time for environmental isolates of *M. aeruginosa* cultured in BG-11 medium as 2.8 days. In the current study *M. aeruginosa* PCC7813 was placed in artificial fresh water which contained none of the main nutrients required for growth, which can explain the slower doubling rate. Another factor that will affect the growth rate of *M. aeruginosa* is the initial inoculation cell density. In the current study initial cell density was $15x10^6$ cells mL^{-1} in 30 mL, which represents a very high inoculation cell density. In a laboratory study Dunn and Manoylov (2016) have demonstrated that *M. aeruginosa* UTEX2385 does not grow as rapidly with a higher ($7x10^5$ cells mL^{-1})

initial inoculation cell density compared to a lower ($1x10^5$ cells mL^{-1}) one in Bolds medium under laboratory conditions. No extracellular MC-LY was detected over the entire experimental period in neither the treatment samples or controls. This can be explained by the low intracellular concentrations of MC-LY (0.06 µg mL^{-1}) present.

4. Conclusions

In the current study we have demonstrated that a simple photocatalytic system of recycled, TiO_2 coated, porous, foamed glass beads with low level UV irradiation supplied by UV emitting LEDs can successfully inhibit cyanobacterial growth and eliminate released microcystins. The design of the treatment system is readily scalable. The housing of the beads can be increased in size to contain more TiO_2-coated beads and the application of waterproof UV-LEDs in long strips attached to the side of the bead housing would facilitate the required UV irradiation. These LEDs may be powered by integrated floating solar panels that would provide a self-contained and sustainable treatment system.

The proposed treatment system:

- is energy efficient due to the use of UV emitting LEDs requiring a lower energy in-put compared to conventional bulb light sources (mW power input compared to W)
- could be powered *in situ* by photovoltaic cells to further increase the energy efficiency
- does not exacerbate the treatment challenge of, especially dissolved, cyanobacterial secondary metabolite and intracellular organic material by photocatalytically removing intracellular toxins

- represents a "green" treatment option through the use of recycled materials, catalyst, and low-energy LEDs (which could be further enhanced by the application of photovoltaic cells).

5. Acknowledgements

The authors would like to acknowledge the Engineering and Physical Sciences Research Council (EPSRC) for funding this research [EP/P029280/1]. As per EPSRC requirements, the data will be made publicly available on the Robert Gordon University's repository, OpenAIR@RGU. Len Montgomery is appreciated for proof-reading the manuscript.

6. References

Akkanen, J., Kukkonen, J.V.K., 2003. Measuring the bioavailability of two hydrophobic organic compounds in the presence of dissolved organic matter. Environ. Toxicol. Chem. 22, 518–524. https://doi.org/10.1897/1551-5028(2003)022<0518:MTBOTH>2.0.CO;2

Bishop, W.M., Lynch, C.L., Willis, B.E., Cope, W.G., 2017. Copper-Based Aquatic Algaecide Adsorption and Accumulation Kinetics: Influence of Exposure Concentration and Duration for Controlling the Cyanobacterium *Lyngbya wollei*. Bull. Environ. Contam. Toxicol. 99, 365–371. https://doi.org/10.1007/s00128-017-2134-2

Chow, C.W.K., Drikas, M., House, J., Burch, M.D., Velzeboer, R.M.A., 1999. The impact of conventional water treatment processes on cells of the cyanobacterium *Microcystis aeruginosa*. Water Res. 33, 3253–3262. https://doi.org/10.1016/S0043-1354(99)00051-2

Cornish, B.J.P., Lawton, L. A., Robertson, P.K.J., 2000. Hydrogen peroxide

enhanced photocatalytic oxidation of microcystin-LR using titanium dioxide. Appl. Catal. B Environ. 25, 59–67. https://doi.org/10.1016/S0926-3373(99)00121-6

Daly, R.I., Ho, L., Brookes, J.D., 2007. Effect of chlorination on *Microcystis aeruginosa* cell integrity and subsequent microcystin release and degradation. Environ. Sci. Technol. 41, 4447–4453. https://doi.org/10.1021/es070318s

De Julio, M., Fioravante, D.A., De Julio, T.S., Oroski, F.I., Graham, N.J.D., 2010. A methodology for optimising the removal of cyanobacteria cells from a brazilian eutrophic water. Brazilian J. Chem. Eng. 27, 113–126. https://doi.org/10.1590/S0104-66322010000100010

Drikas, M., Chow, C.W.K., House, J., Burch, M., 2001. Using coagulation, flocculation and settling to remove toxic cyanobacteria. J. Am. Water Work. Assoc. 100–111.

Dunn, R.M., Manoylov, K.M., 2016. The Effects of Initial Cell Density on the Growth and Proliferation of the Potentially Toxic Cyanobacterium *Microcystis aeruginosa.* J. Environ. Prot. 07, 1210–1220. https://doi.org/10.4236/jep.2016.79108

Fagan, R., McCormack, D.E., Dionysiou, D.D., Pillai, S.C., 2016. A review of solar and visible light active TiO2 photocatalysis for treating bacteria, cyanotoxins, and contaminants of emerging concern. Mater. Sci. Semicond. Process 42(1), 2-14.

Fotiou, T., Triantis, T.M., Kaloudis, T., Pastrana-Martinez, L.M., Likodimos, V., Falaras, P., Silva, A.M.T., Hiskia, A., 2013. Photocatalytic degradation of microcystin-LR and off-odor compounds in water under UV-A and solar light with nanostructured photocatalyst based on reduced graphene oxide-TiO_2

composite. Identification of intermediate products. Ind. Eng. Chem. Res. 52(39), 13991-14000.

García-Villada, L., Rico, M., Altamirano, M., Sánchez-Martín, L., López-Rodas, V., Costas, E., 2004. Occurrence of copper resistant mutants in the toxic cyanobacteria *Microcystis aeruginosa*: Characterisation and future implications in the use of copper sulphate as algaecide. Water Res. 38, 2207–2213. https://doi.org/10.1016/j.watres.2004.01.036

Grassian, V.H., O'Shaughnessy, P.T., Adamcakova-Dodd, A., Pettibone, J.M., Thorne, P.S., 2007. Inhalation exposure study of Titanium dioxide nanoparticles with a primary particle size of 2 to 5 nm. Environ. Health Perspect. 115, 397–402. https://doi.org/10.1289/ehp.9469

Greenfield, D.I., Duquette, A., Goodson, A., Keppler, C.J., Williams, S.H., Brock, L.M., Stackley, K.D., White, D., Wilde, S.B., 2014. The Effects of Three Chemical Algaecides on Cell Numbers and Toxin Content of the Cyanobacteria *Microcystis aeruginosa* and *Anabaenopsis* sp. Environ. Manage. 54, 1110–1120. https://doi.org/10.1007/s00267-014-0339-2

Gunaratne, H.Q.N., Pestana, C.J., Skillen, N., Hui, J., Saravanan, S., Edwards, C., Irvine, J.T.S., Robertson, P.K.J., Lawton, L.A., 2020. 'All in one' photo-reactor pod containing TiO_2 coated glass beads and LEDs for continuous photocatalytic destruction of cyanotoxins in water. Environ. Sci. Water Res. Technol. 6, 945-950. https://doi.org/10.1039/c9ew00711c

Harke, M.J., Steffen, M.M., Gobler, C.J., Otten, T.G., Wilhelm, S.W., Wood, S.A., Paerl, H.W., 2016. A review of the global ecology, genomics, and biogeography of the toxic cyanobacterium, *Microcystis* spp. Harmful Algae 54, 4–20. https://doi.org/10.1016/j.hal.2015.12.007

Heering, W., 2004. UV-sources - Basics, Properties and Applications. Int. Ultrav.

Assoc. 6, 7–13.

Heinlaan, M., Ivask, A., Blinova, I., Dubourguier, H.C., Kahru, A., 2008. Toxicity of nanosized and bulk ZnO, CuO and TiO_2 to bacteria *Vibrio fischeri* and crustaceans *Daphnia magna* and *Thamnocephalus platyurus*. Chemosphere 71, 1308–1316. https://doi.org/10.1016/j.chemosphere.2007.11.047

Jančula, D., Maršálek, B., 2011. Critical review of actually available chemical compounds for prevention and management of cyanobacterial blooms. Chemosphere 85, 1415–1422. https://doi.org/10.1016/j.chemosphere.2011.08.036

Kinley, C.M., Hendrikse, M., Calomeni, A.J., Geer, T.D., Rodgers, J.H., 2018. Solar Photocatalysis Using Fixed-Film TiO_2 for Microcystins from Colonial *Microcystis aeruginosa*. Water. Air. Soil Pollut. 229, 167. https://doi.org/10.1007/s11270-018-3791-4

Komárek, J., Komárková, J., 2002. Review of the European *Microcystis* morphospecies (Cyanoprokaryotes) from nature. Fottea 2, 1–24.

Lawton, L.A., Robertson, P.K.J., Cornish, B.J.P.A., Marr, I.L., Jaspars, M., 2003. Processes influencing surface interaction and photocatalytic destruction of microcystins on titanium dioxide photocatalysts. J. Catal. 213, 109–113. https://doi.org/10.1016/S0021-9517(02)00049-0

Li, L., Gao, N., Deng, Y., Yao, J., Zhang, K., 2012. Characterization of intracellular & extracellular algae organic matters (AOM) of *Microcystic aeruginosa* and formation of AOM-associated disinfection byproducts and odor & taste compounds. Water Res. 46, 1233–1240. https://doi.org/10.1016/j.watres.2011.12.026

Liao, X., Wang, X., Zhao, K., Zhou, M., 2009. Photocatalytic inhibition of cyanobacterial growth using silver-doped TiO_2 under UV-C light. J. Wuhan

573 Univ. Technol. Mater. Sci. Ed. 24, 402–408.
574 https://doi.org/10.1007/s11595-009-3402-8
575 Liu, I., Lawton, L.A., Bahnemann, D.W., Liu, L., Proft, B., Robertson, P.K.J.,
576 2009. The photocatalytic decomposition of microcystin-LR using selected
577 titanium dioxide materials. Chemosphere 76, 549–553.
578 https://doi.org/10.1016/j.chemosphere.2009.02.067
579 Liu, Y., Yang, S., Hong, J., Sun, C., 2007. Low-temperature preparation and
580 microwave photocatalytic activity study of TiO_2-mounted activated carbon. J.
581 Hazard. Mater. 142, 208–215.
582 https://doi.org/10.1016/j.jhazmat.2006.08.020
583 Mills, A., Wang, J., Crow, M., 2006. Photocatalytic oxidation of soot by P25 TiO_2
584 films. Chemosphere 64, 1032–1035.
585 https://doi.org/10.1016/j.chemosphere.2006.01.077
586 Ou, H., Gao, N., Deng, Y., Qiao, J., Wang, H., 2012. Immediate and long-term
587 impacts of UV-C irradiation on photosynthetic capacity, survival and
588 microcystin-LR release risk of Mircocystis aeruginosa. Water Res. 46, 1241-
589 1250. https://doi.org/10.1016/j.watres.2011.12.025
590 Pelaez, M., de la Cruz, A.A., O'Shea, K., Falaras, P., Dionysiou, D.D., 2011.
591 Effects of water parameters on the degradation of microcystin-LR under
592 visible light-activated TiO_2 photocatalyst. Water Res. 45, 3787–3796.
593 https://doi.org/10.1016/j.watres.2011.04.036
594 Pestana, C.J., Edwards, C., Prabhu, R., Robertson, P.K.J., Lawton, L.A., 2015.
595 Photocatalytic degradation of eleven microcystin variants and nodularin by
596 TiO_2 coated glass microspheres. J. Hazard. Mater. 300, 347–353.
597 https://doi.org/10.1016/j.jhazmat.2015.07.016
598 Pinho, L.X., Azevedo, J., Brito, A., Santos, A., Tamagnini, P., Vilar, V.J.P.,

599 Vasconcelos, V.M., Boaventura, R.A.R., 2015. Effect of TiO_2 photocatalysis
600 on the destruction of *Microcystis aeruginosa* cells and degradation of
601 cyanotoxins microcystin-LR and cylindrospermopsin. Chem. Eng. J. 268,
602 144–152. https://doi.org/10.1016/j.cej.2014.12.111
603 Spoof, L., Catherine, A., 2017. Appendix 3, tables of microcystins and
604 nodularins, in: Meriluoto, J., Spoof, L., Codd, G.A. (Eds.), Handbook of
605 Cyanobacterial Monitoring and Cyanotoxin Analysis. John Wiley & Sons,
606 Chichester, UK, pp. 526–537.
607 Stanier, R.Y., Kunisawa, R., Mandel, M., Cohen-Bazire, G., 1971. Purification and
608 properties of unicellular blue-green algae (order Chroococcales). Bacteriol.
609 Rev. 35, 171–205. https://doi.org/10.1128/mmbr.35.2.171-205.1971
610 Varuni, P., Menon, S.N., Menon, G.I., 2017. Phototaxis as a Collective
611 Phenomenon in Cyanobacterial Colonies. Sci. Rep. 7, 1–10.
612 https://doi.org/10.1038/s41598-017-18160-w
613 Velzeboer, R., Drikas, M., Donati, C., Burch, M., Steffensen, D., 1995. Release of
614 Geosmin by *Anabaena circinalis* Following Treatment with Aluminum Sulfate.
615 Water Sci. Technol. 31, 187–194.
616 Wang, J., Zhou, G., Chen, C., Yu, H., Wang, T., Ma, Y., Jia, G., Gao, Y., Li, B.,
617 Sun, J., Li, Y., Jiao, F., Zhao, Y., Chai, Z., 2007. Acute toxicity and
618 biodistribution of different sized titanium dioxide particles in mice after oral
619 administration. Toxicol. Lett. 168, 176–185.
620 https://doi.org/10.1016/j.toxlet.2006.12.001
621 Wang, Xin, Wang, Xuejiang, Zhao, J., Song, J., Wang, J., Ma, R., Ma, J., 2017.
622 Solar light-driven photocatalytic destruction of cyanobacteria by F-Ce-
623 TiO_2/expanded perlite floating composites. Chem. Eng. J. 320, 253–263.
624 https://doi.org/10.1016/j.cej.2017.03.062

WHO, 2017. Guidelines for Drinking-water Quality: fourth edition incorporating the first addendum. Geneva.

Wilson, A.E., Wilson, W.A., Hay, M.E., 2006. Intraspecific variation in growth and morphology of the bloom-forming cyanobacterium *Microcystis aeruginosa*. Appl. Environ. Microbiol. 72, 7386–7389. https://doi.org/10.1128/AEM.00834-06

Wolfe, R.L., 1990. Ultraviolet disinfection of potable water: Current technology and research needs. Environ. Sci. Technol. 24, 768–773. https://doi.org/10.1021/es00076a001

Zhu, X., Chang, Y., Chen, Y., 2010. Toxicity and bioaccumulation of TiO_2 nanoparticle aggregates in *Daphnia magna.* Chemosphere 78, 209–215. https://doi.org/10.1016/j.chemosphere.2009.11.013

Zilliges, Y., Kehr, J.C., Meissner, S., Ishida, K., Mikkat, S., Hagemann, M., Kaplan, A., Börner, T., Dittmann, E., 2011. The cyanobacterial hepatotoxin microcystin binds to proteins and increases the fitness of *Microcystis* under oxidative stress conditions. PLoS One 6(3): e17615. https://doi.org/10.1371/journal.pone.0017615

Supplementary Information:

Photocatalytic removal of the cyanobacterium *Microcystis aeruginosa* PCC7813 and four microcystins by TiO_2 coated porous glass beads with UV-LED irradiation

Carlos J. Pestana[a*], Jolita Portela Noronha[a,b], Jianing Hui[c], C. Edwards[a], H. Q. Nimal Gunaratne[d], John T.S. Irvine[c], Peter K.J. Robertson[d], José Capelo-Neto[b], Linda A. Lawton[a]

[a] School of Pharmacy and Life Sciences, Robert Gordon University, Aberdeen, United Kingdom

[b] Department of Hydraulic and Environmental Engineering, Federal University of Ceará, Fortaleza, Brazil

[c] School of Chemistry, University of St Andrews, St Andrews, United Kingdom

[d] School of Chemistry and Chemical Engineering, Queen's University, Belfast, United Kingdom

S1 Characterization of porous foamed glass beads and TiO_2 coating

Virgin (as received from Dennert Poraver GmbH, Germany) and TiO_2 coated porous foamed glass beads were characterized by SEM-EDS analysis (Scios DualBeam, Thermo Scientific) and X-ray diffraction analysis (XRD, Empyrean X-ray diffractometer, Malvern Panalytical, UK; X-ray diffractometer was operated in reflection mode (Cu Kα1)) (figure S1). The porous foamed nature of the virgin glass beads can clearly be discerned (figure S1 A and B). The surface of the beads is slightly undulating with exposed areas of the foamed material, but otherwise smooth (figure S1 A and C). Silica, sodium, calcium and oxygen are the main constituents of the beads, as would be expected from glass material (figure S1 D). The other elements present are most likely due to the recycled nature of the source material. After the coating process the surface of the beads is less undulating and presents with almost complete coverage of the surface with catalyst. The EDS analysis (figure S1 F) confirms more than 11% Ti (atomic ratio) was found on coated beads surface. Phases of coating layer were determined by X-ray diffraction (XRD, figure S1 G). Anatase and rutile phases of the TiO_2 P25 precursor remained unchanged, without introducing any other impurities during processing. The BET surface area of the TiO_2 coated glass beads is 2.49 $m^2 g^{-1}$, while the uncoated beads present a surface area of 0.15 $m^2 g^{-1}$. The thickness of the TiO_2 layer ranged from 0.5 µm to 5 µm. It is not uniform because the surface of the expanded beads is not regular, causing a thicker deposition layer in the lower spots of the morphology. The 10% (w/w) coating was determined to be the best compromise between a complete coating of the beads (as determined by visual analysis by SEM) and avoiding shedding of the material.

Figure S1: Characterization of the virgin and TiO_2 coated porous foamed glass beads. (A) surface of the glass bead (35x magnification); (B) cross section through virgin glass bead showing air pockets due the foamed nature of the material (35x magnification); (C) surface morphology of the virgin porous glass beads (50,000x magnification); (D) Elemental characterization of porous foamed glass beads as determined by EDS analysis; (E) Surface morphology of porous foamed glass beads after repeated coating with P25 TiO_2 (final 10% w/w); (F) elemental characterization of TiO_2 coated porous foamed glass beads as determined by EDS analysis confirming the presence of titanium on the surface of the beads; (G) x-ray diffraction analysis confirming that the TiO_2 P25 precursor remains unchanged after coating, presenting characteristic peaks for the anatase and rutile phases of P25.

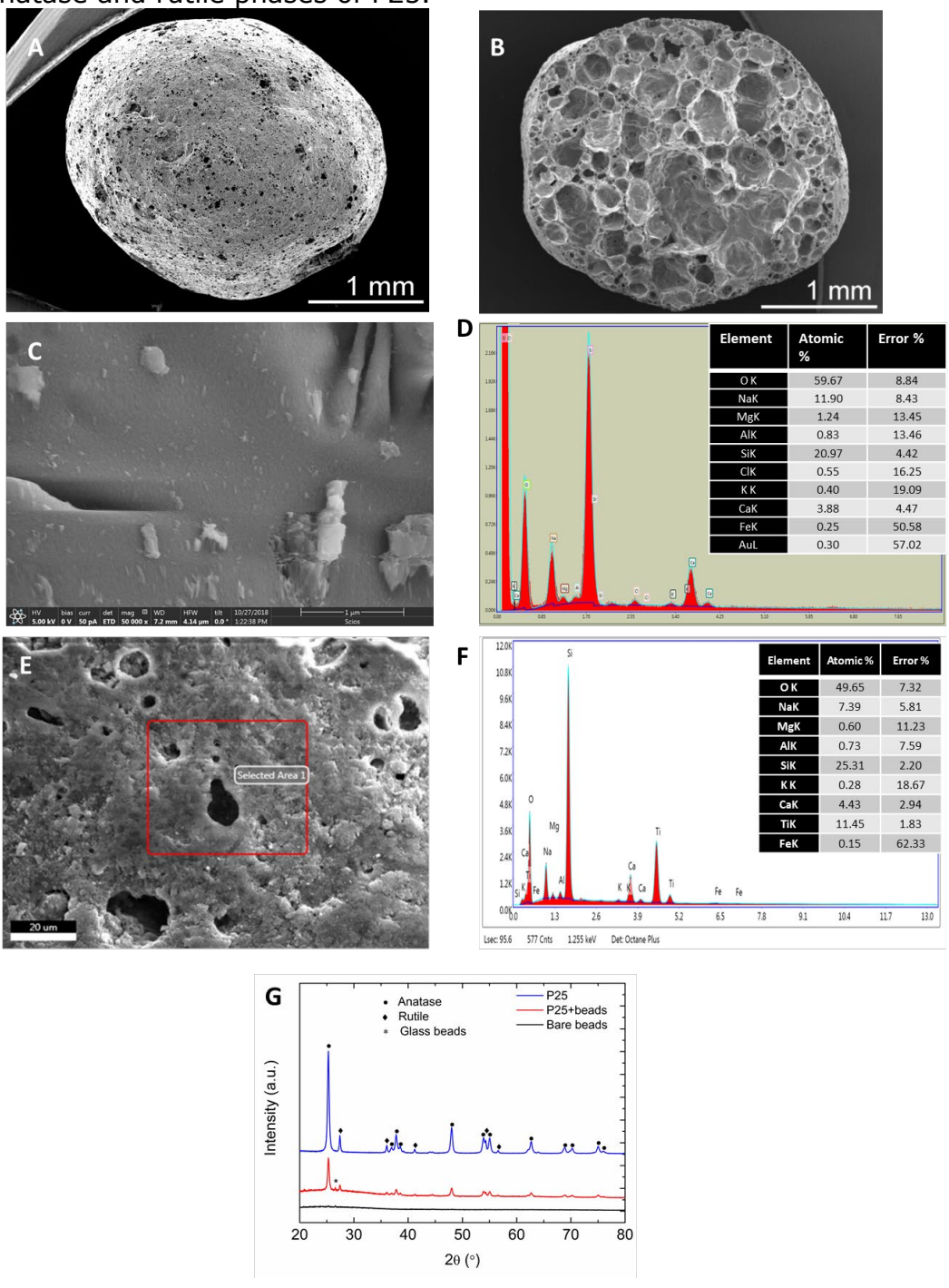

With a lower TiO_2 loading amount complete surface coverage was not achieved, thus repeated coating steps were performed. On the other hand, the catalyst shedding occurred at higher loading amounts. Thus, 10% (w/w) was determined iteratively as the optimal loading with enough catalyst to allow for complete coverage of the whole surface of the glass beads while, at the same time, maintaining sufficient robustness of the coating layer.